

# On the Overshooting Effect in EXIT Charts of Iterative Source-Channel Decoding

M. Adrat, M. Antweiler  
FKIE Communication Systems  
Fraunhofer-Gesellschaft  
Wachtberg, Germany  
marc.adrat@fkie.fraunhofer.de

L. Schmalen, P. Vary  
Inst. of Comm. Systems and Data Processing  
RWTH University  
Aachen, Germany  
schmalen@ind.rwth-aachen.de

T. Clevorn  
Design Center NRW  
Infineon Technologies AG  
Duisburg, Germany  
thorsten.clevorn@infineon.com

**Abstract**—Source codec parameters determined by modern source encoders are usually very sensitive to noise on the transmission link. Natural residual redundancy of these parameters can be utilized by *Soft Decision Source Decoding* (SDSD) [1] to increase the error resistance. Serially concatenating *Forward Error Correction* (FEC) and SDSD leads to a *Iterative Source-Channel Decoding* (ISCD) scheme [2, 3] which offers further improvements in robustness. ISCD exploits natural residual source redundancy by SDSD and artificial channel coding redundancy due to FEC in an iterative Turbo-like process [4, 5]. The convergence behavior of ISCD schemes can be analyzed by *EXtrinsic Information Transfer* (EXIT) charts [6, 7].

However, if an advanced ISCD system design [8–11] is applied, offering incremental quality improvements for many iterations, the EXIT curves for SDSD do not specify a tight bound for the decoding trajectory anymore. In the initial iterations, the decoding trajectory “overshoots” the EXIT curves of SDSD, e.g. [12, 13].

In this paper, we give reasons for this overshooting effect. In addition, we propose a novel solution for determining the EXIT curve of SDSD which allows a more precise convergence analysis.

## I. ITERATIVE SOURCE-CHANNEL DECODING

In this section, we will introduce the considered overall transmission scheme first. After that, in Section I-B we will briefly review those parts of the *Iterative Source-Channel Decoding* (ISCD) algorithm [2, 3] which are of relevance to understand the “overshooting” effect. The concept of EXIT charts [6] and the “overshooting” effect itself will be explained in detail in Section II. Finally, we propose our novel solution for determining more precise EXIT curves for *Soft Decision Source Decoding* (SDSD) [1, 12]. The extended capabilities will be demonstrated by simulation in Section III.

### A. Transmitter

Let us introduce the considered transmission scheme first (see Figure 1). We assume that a parametric source encoder extracts a *parameter set*  $\underline{v}_k$  from the  $k$ -th segment of the input signal. The set  $\underline{v}_k$  shall consist of  $M$  scalar *source codec parameters*  $v_{m,k}$ ,  $m = 1, \dots, M$ . The  $M$  source codec parameters  $v_{m,k}$  are individually quantized to *quantizer reproduction levels*  $\bar{v}_{m,k} \in \mathbb{V}_m$ . The *quantizer codebooks*  $\mathbb{V}_m$  of size  $|\mathbb{V}_m|$  are time invariant. Usually,  $w_m = \log_2(|\mathbb{V}_m|)$  quantifies the length of the *bit pattern*  $\mathbf{x}_{m,k} = \Phi_m(\bar{v}_{m,k})$  after index assignment and bit mapping, i.e.,  $\mathbf{x}_{m,k}$  consists of  $w_m$  (bipolar) bits  $x_{m,k}(l) \in \{+1, -1\}$  with  $l = 1, \dots, w_m$ . The bit patterns are assumed to exhibit some natural residual source redundancy in terms of correlation in time  $k$  which can

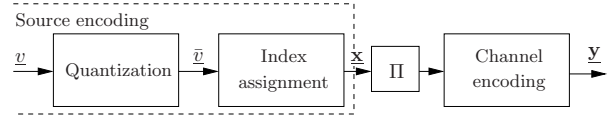


Fig. 1. Block diagram for Encoding Scheme of Transmission System

be quantified by the *conditional probability mass function*<sup>1</sup>  $P(\mathbf{x}_k | \mathbf{x}_{k-1})$ . The complete frame of bit patterns representing the set  $\underline{v}_k$  is denoted as  $\underline{\mathbf{x}}_k$ .

For convenience, we assume in the following that the quantizer codebooks and index assignments are the same for all  $M$  source codec parameters  $v_{m,k}$ , i.e. we can write  $\mathbb{V} = \mathbb{V}_m$ ,  $w = w_m$ , and  $\Phi(\cdot) = \Phi_m(\cdot)$  for all  $m = 1, \dots, M$ . Moreover, wherever possible without risk of confusion we skip the indices for time  $k$ , position  $m$ , and bit  $l$ .

Figure 2 illustrates the relation between a single bit  $x_k$ , a bit pattern  $\mathbf{x}_k$ , and a frame  $\underline{\mathbf{x}}_k$ .

Next, a block-type *bit interleaver*  $\Pi$  is applied jointly to  $T$  consecutive frames  $\underline{\mathbf{x}}_{k+\Lambda-T+1}, \dots, \underline{\mathbf{x}}_k, \dots, \underline{\mathbf{x}}_{k+\Lambda}$  (in Fig. 2 we set  $\Lambda = T-1$ ). The index  $\Lambda$  denotes the maximum tolerable look-ahead. Note, this will introduce a latency of up to  $\Lambda$  frames which can be avoided by setting  $T = 1$  as done in Section III. The overall *interleaver size* accumulates to  $M w T$ .

In the following, the notation will always refer to the deinterleaved domain if there is no risk of confusion.

Finally, a channel code of *code rate*  $r$  expands the series of

<sup>1</sup>The ISCD algorithm can easily be extended to consider cross-correlation in adjacent positions  $m$ , i.e. to  $P(\mathbf{x}_{m,k} | \mathbf{x}_{m-1,k})$ , as well. However, in this case an “overshooting” effect does not appear (see reason given in Section II).

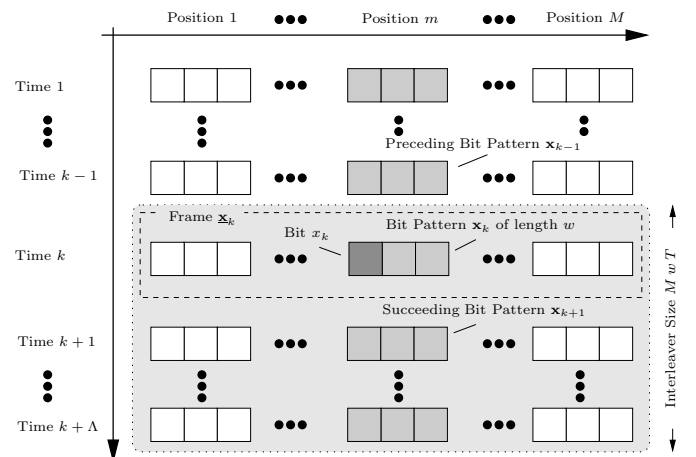


Fig. 2. Relation between Bit  $x_k$ , Bit Pattern  $\mathbf{x}_k$  & Frame  $\underline{\mathbf{x}}_k$  (here  $\Lambda = T-1$ )

$T$  interleaved consecutive sets  $\underline{x}$  of bit patterns to a sequence  $\underline{y}$  of size  $MwT/r$  with code bits  $y(l)$ ,  $l = 1, \dots, MwT/r$ . In this paper, we restrict our considerations to convolutional codes. Note, if a convolutional code with memory  $J$  shall terminate to a predefined state, the number of code bits  $y$  increases to  $(MwT + J)/r$  due to the  $J$  termination bits.

The individual code bits  $y$  are BPSK-modulated (*binary phase shift keying*), i.e. mapped to code symbols  $\{+1, -1\}$  before transmission. The energy  $E_s$  per transmitted BPSK-modulated code symbol is constantly  $E_s = 1$ . To simplify matters, the transmission channel is considered as a memoryless AWGN (*Additive White Gaussian Noise*) channel.

### B. Receiver with Iterative Source-Channel Decoding

After transmitting each code symbol  $y$  over the AWGN channel a possibly noisy value  $z = y + n$  with  $z \in \mathbb{R}$  is received. The reliability of the channel transmission can be expressed in terms of a channel-related *log-likelihood ratio*  $L(z|y)$  (short *L-value*) [5]

$$L(z|y) = 4a \cdot E_s/N_0 \cdot z, \quad (1)$$

The term  $N_0/2$  denotes the power spectral density of the effective real-valued AWGN  $n$ . Time variant signal fading can easily be considered by the fading factor  $a$  (here,  $a = 1$ ).

The aim of *iterative source-channel decoding* (ISCD) is to jointly exploit the channel-related *L-values* of (1), the artificial channel coding redundancy as well as the natural residual source redundancy. The optimum bit decision should be based on the *a posteriori L-value*  $L(x|\underline{z})$  for a single data bit  $x$  given the complete history of received sequences  $\underline{z}$ . These *a posteriori L-values* can be separated according to Bayes' Theorem into up to four additive terms, if a memoryless channel is assumed (see e.g. [2, 7, 9, 12])

$$L(x|\underline{z}) = L(z|x) + L(x) + L_{\text{FEC}}^{\text{[ext],i}}(x) + L_{\text{SDSD}}^{\text{[ext],i}}(x). \quad (2)$$

The first term on the right hand side,  $L(z|x)$ , specifies the bitwise channel-related *L-value* according to (1) if systematic channel encoding is assumed (i.e. if the data bits  $x$  are present in the code sequence  $\underline{y}$ ). In case of a non-systematic channel code we get  $L(z|x) = 0$ . The second term  $L(x)$  quantifies the bitwise *a priori* information which determines whether a data bit  $x = +1$  or  $x = -1$  is more likely. This term can be measured once in advance for a representative signal data base.

The remaining two terms  $L_{\text{FEC}}^{\text{[ext],i}}(x)$  /  $L_{\text{SDSD}}^{\text{[ext],i}}(x)$  mark so-called *extrinsic information* [2, 5] and result from the evaluation of the natural residual source redundancy (labeled with "SDSD") or of the artificial channel coding redundancy (labeled with "FEC"). Two independent terms of *extrinsic L-values* are essential for an iterative Turbo process [4, 5]. In such processes the (de-)interleaved *extrinsic* output of the one decoder serves as (additional) soft input for the other constituent decoder and vice versa. An iterative refinement of both *extrinsic L-values* usually enables step-wise reliability improvements. Here,  $i$  denotes the iteration counter.

Figure 3 shows the block diagram of the receiving side of the transmission system with ISCD.

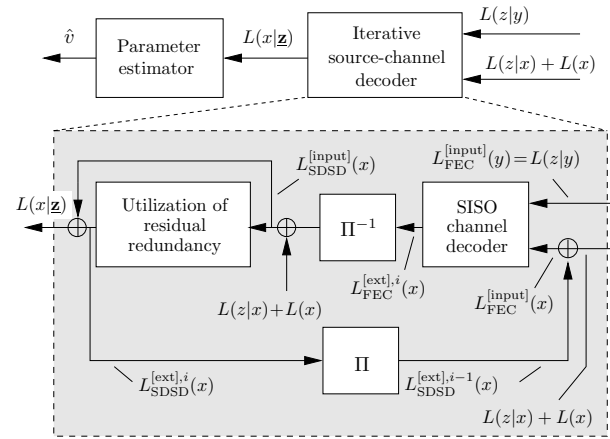


Fig. 3. Block diagram for a receiver with ISCD

### C. Extrinsic *L-value* of SISO Channel Decoding

Concepts how to determine the *extrinsic* output *L-value*  $L_{\text{FEC}}^{\text{[ext],i}}(x)$  of *soft-input / soft-output* (SISO) channel decoding from the channel-related inputs  $L(z|x)$  resp.  $L(z|y)$ , the bit-wise *a priori* information  $L(x)$  and the *extrinsic* information provided by an outer decoder are already well known and not of any further interest for the considerations in this paper. For details we refer the reader to the literature (see e.g. [4, 5]).

### D. Extrinsic *L-value* of Soft Decision Source Decoding

However, the determination rule for the *extrinsic L-value*  $L_{\text{SDSD}}^{\text{[ext],i}}(x)$  of *soft decision source decoding* (SDSD) shall briefly be reviewed next. Later on, this determination rule is essential to understand the "overshooting" effect in the EXIT chart of ISCD.

SDSD utilizes the natural residual source redundancy (see Figure 3). As input for the determination of  $L_{\text{SDSD}}^{\text{[ext],i}}(x)$  for an arbitrary but fixed bit  $x$  serves

$$L_{\text{SDSD}}^{\text{[input]}}(x) = L(z|x) + L(x) + L_{\text{FEC}}^{\text{[ext],i}}(x). \quad (3)$$

The combination of the  $w$  inputs  $L_{\text{SDSD}}^{\text{[input]}}(x_k(l))$ ,  $l = 1, \dots, w$ , of the present bit pattern  $\mathbf{x}_k$  as well as the residual redundancy in terms of the conditional probability mass function  $P(\mathbf{x}_k|\mathbf{x}_{k-1})$  allows us to compute the so-called *innovation*

$$\gamma_k(\mathbf{x}_k, \mathbf{x}_{k-1}) = P(\mathbf{x}_k|\mathbf{x}_{k-1}) \cdot \exp \sum_{l=1}^w \frac{x_k(l)}{2} \cdot L_{\text{SDSD}}^{\text{[input]}}(x_k(l)). \quad (4)$$

The mutual dependencies of the entire sequence of bit patterns  $\mathbf{x}_k$  from the very beginning up to the maximum acceptable look-ahead  $k + \Lambda$  can efficiently be considered by a recursive *forward-backward* algorithm [8, 14, 15]

$$\alpha_k(\mathbf{x}_k) = \sum_{\mathbf{x}_{k-1}} \gamma_k(\mathbf{x}_k, \mathbf{x}_{k-1}) \cdot \alpha_{k-1}(\mathbf{x}_{k-1}) \quad (5)$$

$$\beta_k(\mathbf{x}_k) = \sum_{\mathbf{x}_{k+1}} \gamma_{k+1}(\mathbf{x}_{k+1}, \mathbf{x}_k) \cdot \beta_{k+1}(\mathbf{x}_{k+1}). \quad (6)$$

The term  $\alpha_k(\mathbf{x}_k)$  denotes the *forward* recursion and  $\beta_k(\mathbf{x}_k)$  the *backward* recursion. The summations in (5) and (6) run over all  $2^w = |\mathcal{V}|$  possible realizations of  $\mathbf{x}_{k-1}$  resp.  $\mathbf{x}_{k+1}$ .

Determination rule for the *extrinsic*  $L$ -value of *Soft Decision Source Decoding*:

$$L_{\text{SDSD}}^{[\text{ext}]}(x) = \log \frac{\sum_{\mathbf{x}_k^{[\text{ext}]}} \beta_k(\mathbf{x}_k^{[\text{ext}]}, x_k = +1) \cdot \sum_{\mathbf{x}_{k-1}} \gamma_k^{[\text{ext}]}(\mathbf{x}_k^{[\text{ext}]}, \mathbf{x}_{k-1} | x_k = +1) \cdot \alpha_{k-1}(\mathbf{x}_{k-1})}{\sum_{\mathbf{x}_k^{[\text{ext}]}} \beta_k(\mathbf{x}_k^{[\text{ext}]}, x_k = -1) \cdot \sum_{\mathbf{x}_{k-1}} \gamma_k^{[\text{ext}]}(\mathbf{x}_k^{[\text{ext}]}, \mathbf{x}_{k-1} | x_k = -1) \cdot \alpha_{k-1}(\mathbf{x}_{k-1})} \quad (7)$$

As initial values serve  $\alpha_1(\mathbf{x}_1) = P(\mathbf{x})$  (probability distribution of  $\mathbf{x}$ ) and  $\beta_{k+\Lambda}(\mathbf{x}_{k+\Lambda}) = 1$ .

Combining the *forward-backward* recursions  $\alpha_k(\mathbf{x}_k)$  and  $\beta_k(\mathbf{x}_k)$  and a reduced form (explanation follows below) for the *innovation*  $\gamma_k^{[\text{ext}]}(\mathbf{x}_k^{[\text{ext}]}, \mathbf{x}_{k-1} | x_k)$  yields the overall determination rule (7) for  $L_{\text{SDSD}}^{[\text{ext}]}(x)$ .

In (7) the term  $\mathbf{x}_k^{[\text{ext}]}$  stands for the bit pattern  $\mathbf{x}_k$  excluding the data bit  $x_k(l)$  under consideration. Thus, the subpattern  $\mathbf{x}_k^{[\text{ext}]}$  is of length  $w - 1$  and offers  $2^{w-1} = |\mathbb{V}|/2$  possible realizations (see outer summation in (7)). The subset in the numerator is given by those  $\mathbf{x}_k^{[\text{ext}]}$  of  $\mathbf{x}_k$  with  $x_k(l) = +1$  and in the denominator for  $x_k(l) = -1$  respectively.

Figure 4 illustrates the relation between data bit  $x_k(l)$ , the subpattern  $\mathbf{x}_k^{[\text{ext}]}$  as well as preceding patterns  $\mathbf{x}_1, \dots, \mathbf{x}_{k-1}$  and succeeding patterns  $\mathbf{x}_{k+1}, \dots, \mathbf{x}_{k+\Lambda}$ .

In order to disregard the data bit  $x_k(l_x)$  under consideration (dark gray element) it needs to be excluded from (7). This can be done by defining a reduced counterpart to the *innovation* (4) in terms of

$$\gamma_k^{[\text{ext}]}(\mathbf{x}_k^{[\text{ext}]}, \mathbf{x}_{k-1} | x_k) = P(\mathbf{x}_k^{[\text{ext}]} | x_k, \mathbf{x}_{k-1}) \cdot \exp \sum_{l=1, l \neq l_x}^w \frac{x(l)}{2} \cdot L_{\text{SDSD}}^{[\text{input}]}(x(l)). \quad (8)$$

Note, the bit under consideration is explicitly excluded from the summation in the second line.

As shown in Figure 4 the contribution of the *reduced innovation* (8) to the *extrinsic*  $L$ -value of data bit  $x_k(l)$  comes mainly from the subpattern  $\mathbf{x}_k^{[\text{ext}]}$  as well as in combination with the *forward* recursion  $\alpha_{k-1}(\mathbf{x}_{k-1})$  from preceding patterns. Additional knowledge comes from the *backward* recursion  $\beta_k(\mathbf{x}_k)$ .

### E. MMSE Parameter Estimation of Source Codec Parameters

After several iterative refinements of  $L_{\text{FEC}}^{[\text{ext}]}(x)$  and  $L_{\text{SDSD}}^{[\text{ext}]}(x)$  the bit-level *a posteriori*  $L$ -values of (2) are used for estimating the parameters  $\hat{v}$  (see Figure 3). Usually, the *minimum mean squared error* (MMSE) serves as fidelity criterion, such that the *parameter signal-to-noise ratio* (SNR) will be maximized. It quantifies the mean signal power  $E\{|v|^2\}$  divided by the mean squared distortion  $E\{|v - \hat{v}|^2\}$ ,

$$\text{parameter SNR [dB]} = 10 \log_{10} \frac{E\{|v|^2\}}{E\{|v - \hat{v}|^2\}}. \quad (9)$$

The expected values  $E\{\cdot\}$  are evaluated over all time instants  $k$  and positions  $m = 1, \dots, M$ .

## II. OVERSHOOTING EFFECT IN EXIT CHART

### A. Determination of EXIT Curves & EXIT Charts

In order to predict the convergence behavior of iterative processes, a powerful method called *EXIT chart* has been

proposed in [6] which applies the *mutual information* measure to the input/output relations of the individual constituent soft-input/soft-output decoders. On one hand, information exhibited by the (a priori) *input*  $L$ -value  $L^{[\text{apri}]}(x)$ , and on the other hand, information comprised in the *extrinsic* output  $L$ -values  $L^{[\text{ext}]}(x)$  after soft-output decoding is closely related to the information content of the originally transmitted data bits  $x$ .

With respect to the *mutual information* measure the input/output relations can be quantified by  $\mathcal{I}(x; L^{[\text{apri}]}(x))$  and  $\mathcal{I}(x; L^{[\text{ext}]}(x))$ . To simplify notation we define:

$\mathcal{I}^{[\text{apri}]}$  quantifies the *mutual information*  $\mathcal{I}(x; L^{[\text{apri}]}(x))$  in the distributions of the data bit  $x$  and the overall *a priori*  $L$ -value  $L(x) + L^{[\text{apri}]}(x)$ .

$\mathcal{I}^{[\text{ext}]}$  denotes the *mutual information*  $\mathcal{I}(x; L^{[\text{ext}]}(x))$  between  $x$  and the *extrinsic information*  $L^{[\text{ext}]}(x)$ .

The *mutual information* measure  $\mathcal{I}^{[\text{ext}]}$  at the output of the decoder depends on the settings applied at the input. Thereby, the channel-related input ratio  $L(z|x)$  is mainly adjusted by the  $E_S/N_0$  value (see (1)). Observations obtained by simulations reveal [6] that the *a priori*  $L$ -value  $L^{[\text{apri}]}(x)$  can be modeled by a Gaussian distributed random variable with variance  $\sigma_L^2 = 8/N_0$  and mean  $\mu_L = \sigma_L/2 \cdot x$ . Since both are adjustable by a single variable  $\sigma_L^2$ , for arbitrary  $\sigma_L^2$  the *a priori* relation  $\mathcal{I}^{[\text{apri}]}$  can immediately be computed [6]. Thus, the EXIT curves  $\mathcal{T}$  of soft-output decoders are defined as [6]

$$\mathcal{I}^{[\text{ext}]} = \mathcal{T}(\mathcal{I}^{[\text{apri}]}, E_S/N_0) \quad (10)$$

If defined settings for  $\mathcal{I}^{[\text{apri}]}$  resp.  $\sigma_L^2$  and for  $E_S/N_0$  are adjusted,  $\mathcal{I}^{[\text{ext}]}$  is quantifiable by means of Monte-Carlo simulations.

Note, in case of channel decoding  $L_{\text{FEC}}^{[\text{apri}]}(x)$  is given by the interleaved  $L_{\text{SDSD}}^{[\text{ext}],i}(x)$ , i.e. by the interleaved *extrinsic*  $L$ -values of SDSD. In case of SDSD,  $L_{\text{SDSD}}^{[\text{apri}]}(x)$  is given by

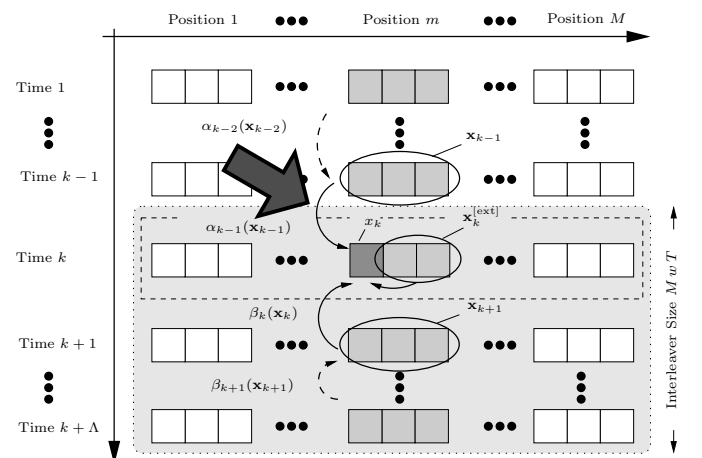


Fig. 4. Illustration for Determination Rule (7) for  $L_{\text{SDSD}}^{[\text{ext}]}(x)$



the deinterleaved  $L_{\text{FEC}}^{[\text{ext}],i}(x)$ . In addition, if a non-systematic<sup>2</sup> channel code is used the EXIT curves of SDDS become independent of  $E_S/N_0$ .

The combination of EXIT curves of two soft-output decoders in a single diagram is referred to as EXIT chart [6]. Note, due to the nested structure of  $L_{\text{FEC}/\text{SDDS}}^{[\text{apri}]}$  and  $L_{\text{SDDS}/\text{FEC}}^{[\text{ext}],i}(x)$  (the output of one serves as input for the other) the axis of the second EXIT curve are swapped. The main contribution of EXIT charts is that an analysis of the convergence behavior of a concatenated scheme is realizable by solely studying the EXIT curves of the single components.

A step curve in between the two EXIT curves is called *decoding trajectory*. Each step represents an iteration. Figure 5 shows two examples for different numbers of iteration  $i$  (for details of simulation settings see Section III).

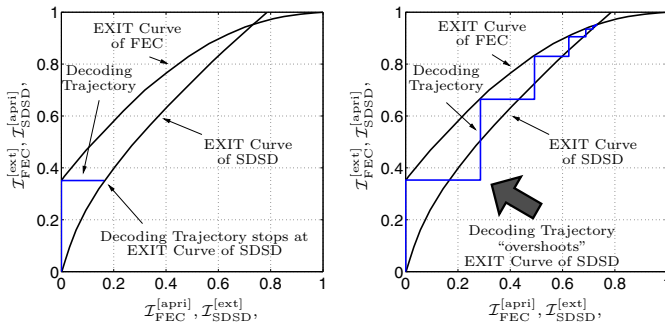


Fig. 5. Example for “Overshooting” Effect (left:  $i = 1$ , right:  $i = 10$ )

It can be seen that for  $i = 1$  (left) the *decoding trajectory* stops at the EXIT curve of SDDS. However, if we increase the number of iterations to e.g.  $i = 10$  (right) the EXIT curve of SDDS does not define a tight bound anymore. It is clearly visible that in this example the *decoding trajectory* overshoots the EXIT curve. The reason will be explained next.

### B. Reason for the Overshooting Effect & Problem Solution

The main reason lies in the process how the EXIT curve of SDDS is determined. As mentioned above, when measuring the *mutual information*  $\mathcal{I}_{\text{SDDS}}^{[\text{ext}]}$  of SDDS the deinterleaved *extrinsic L-values*  $L_{\text{FEC}}^{[\text{ext}],i}(x)$  at the input are approximated by a Gaussian distribution with variance  $\sigma_L^2$  and mean  $\mu_L$ . It has to be pointed out, that (so far) it is common to use the *same* variance and mean for all  $L_{\text{FEC}}^{[\text{ext}],i}(x)$ .

As a consequence, the  $L_{\text{FEC}}^{[\text{ext}],i}(x)$  with the same Gaussian distribution contribute to  $L_{\text{SDDS}}^{[\text{input}]}(x)$  according to (3). Thus, the intermediate results of the *innovation*  $\gamma_k(\mathbf{x}_k, \mathbf{x}_{k-1})$  (see (4)) as well as of the *forward-backward* recursions  $\alpha_k(\mathbf{x}_k)$  and  $\beta_k(\mathbf{x}_k)$  (see (5) and (6)) are based on the same Gaussian distributed process regardless of the time index  $k$ .

However, it can be seen from Figure 4 that the ISCD process runs on interleaver blocks of size  $MwT$ . That means, the

<sup>2</sup>Note, in case of a systematic channel code the serially concatenated ISCD scheme can also be interpreted as a *parallel* concatenated scheme [7]. It depends on the preferences of the system designer whether channel-related knowledge  $L(z|x)$  is considered to be part of  $L_{\text{FEC}}^{[\text{ext}],i}(x)$  or not (cmp. to (3)). The first approach yields a unique EXIT curve for SDDS for all  $E_S/N_0$  while the latter approach results in a selection of EXIT curves [7].

*extrinsic L-values*  $L_{\text{SDDS}}^{[\text{ext}],i}(x)$  of only those data bits  $x$  benefit from the iterations  $i$  which are taken into account by the present interleaver block. The iterative process for all data frames  $\underline{\mathbf{x}}$  preceding the present block (in Figure 4 frames  $\underline{\mathbf{x}}_1, \dots, \underline{\mathbf{x}}_{k-1}$ ) has already been finished, i.e. the maximum number of iterations  $i_{\text{max}}$  has already been reached.

Thus, even though commonly used, the assumption of a single Gaussian distributed process for all input  $L$ -values  $L_{\text{FEC}}^{[\text{ext}],i}(x)$  is not fulfilled in any case. The mismatch can appear at the transition of preceding interleaver blocks to the present interleaver block (marked by an arrow in Figure 4). It can appear in particular in those situations where the maximum number of iterations  $i_{\text{max}}$  carried out on preceding interleaver blocks differs (significantly) from the number of iterations  $i$  applied to the data of the present interleaver block. In the example shown in Figure 5  $i_{\text{max}} = i = 1$  (left subplot) while  $i_{\text{max}} = 10$  greater than  $i = 1$  (right subplot).

To solve this mismatch, we propose to use two separate Gaussian distributed processes. The first one is used in the *classic* way (as described above) for all  $L_{\text{FEC}}^{[\text{ext}],i}(x)$  of the present interleaver block. The second one is applied to the computation of the *forward* recursion  $\alpha_k(\mathbf{x}_k)$  which serves as input to the present interleaver block (i.e.  $\alpha_{k-1}(\mathbf{x}_{k-1})$  in Figure 4, see transition marked by the arrow). In the remainder we set the variance  $\sigma_L^2$  and mean  $\mu$  of the second Gaussian distributed process to such a high value for which a *classic design* would yield  $\mathcal{I}^{[\text{apri}]} \approx 1$  bit. This resembles some kind of *error-free feed “forward”* from preceding interleaver blocks to the present one, i.e. the *new* EXIT curves presented in the following can be considered as an upper bound.

## III. SIMULATION RESULTS

The extended capabilities of the proposed approach to determine the EXIT curve of SDDS using two separate Gaussian distributed processes shall be demonstrated by simulation. However, before introducing details of the simulation settings it needs to be pointed out that, in a Turbo process, *bit interleaving* attracts special attention. *Bit interleaving* has to be realized such that independent *extrinsic information* can be extracted for several iterations  $i$  from both component decoders, SISO channel decoding and *soft decision source decoding*. Therefore, the *bit interleaver* needs to be sufficiently large and properly designed.

### A. Simulation Settings for Experiments A & B

1) *Experiment A*: In a first *Experiment A*, we assume a interleaver block size of  $MwT = 1500$  bits in order to avoid any adverse effect of small interleavers on our simulation results and to allow us to use a pseudo-random interleaver design (*S-random*). This number is split into  $T = 1$  (to avoid any latency),  $w = 3$  bits  $x_k$  per bit pattern  $\mathbf{x}_k$  and  $M = 500$  bit patterns  $\mathbf{x}_k$  per frame  $\underline{\mathbf{x}}_k$ . The source codec parameter conditional probability mass function  $P(\mathbf{x}_k | \mathbf{x}_{k-1})$  shall result from a Gauss-Markov process for the source codec parameters  $v$  (with variance  $\sigma_v^2 = 1$  and auto-correlation  $\rho = 0.9$ ) which are quantized to  $\bar{v}$  by an 8-level Lloyd-Max quantizer and mapped into the bit pattern  $\mathbf{x}$  according to the SOAK1 (*source*

optimized for first order a priori knowledge [13]) index assignment. For  $\rho = 0.9$  and 8-level Lloyd-May quantization the SOAK1 mapping reads  $\{0, 1, \dots, 7\} \rightarrow \{0, 5, 3, 6, 4, 1, 2, 7\}$ .

Channel coding is realized by a terminated memory  $J = 3$ , rate  $r = 1/2$  recursive non-systematic convolutional (RNSC) code with generator polynomial  $G(15/17, 13/17)_8$ .

2) *Experiment B*: In a second *Experiment B*, we consider the same Gauss-Markov process (with  $\sigma_v^2 = 1$  and  $\rho = 0.9$ ) and the same 8-level Lloyd-Max quantizer, but we use a redundant index assignment [10, 11, 15] which maps the 8-levels into a bit pattern  $\mathbf{x}_k$  of length  $w = 6$  bits. This mapping reads  $\{0, 1, \dots, 7\} \rightarrow \{41, 8, 15, 4, 63, 23, 1, 32\}$ . Thus, the interleaver size increases to  $MwT = 3000$  bits. To keep the data rate on the transmission channel constant, we use a terminated memory  $J = 3$ , rate  $r = 1$  RNSC code with generator polynomial  $G(10/17)_8$ .

### B. EXIT Chart & Decoding Trajectory

1) *Experiment A*: Figure 6 shows the corresponding EXIT chart for an AWGN channel with  $E_S/N_0 = -4$  dB.

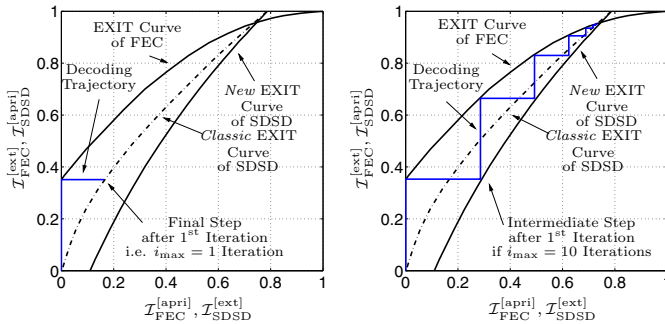


Fig. 6. New EXIT Curve of SDDS outperforms Classic Design for  $i_{\max} = 10$

It can be seen that the proposed approach to consider two separate Gaussian distributed processes to approximate the data of the present as well as of the past interleaver blocks yields a EXIT curve of SDDS which sets precise limits for the decoding trajectory. No “overshooting” occurs anymore. While the *classic* approach provides excellent results for  $i_{\max} = 1$ , the *new* approach yields a tight bound for higher numbers of iteration (here:  $i_{\max} = 10$ ).

2) *Experiment B*: Figure 7 shows the EXIT chart for *Experiment B* again for an AWGN channel with  $E_S/N_0 = -4$  dB.

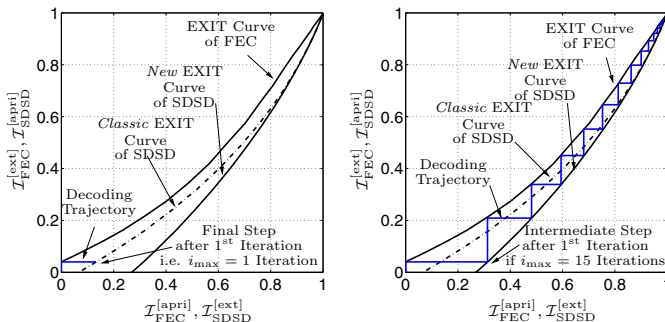


Fig. 7. Benefits of New EXIT Curve of SDDS if compared to Classic Design

*Experiment B* confirms the results of *Experiment A*. All conclusions can be transferred from one to the other experiment. The *classic* EXIT curve of SDDS provides precise results for  $i_{\max} = 1$  only. The *new* EXIT curve yields a tight bound for higher numbers of iteration (here:  $i_{\max} = 15$ ).

### IV. CONCLUSIONS

In this paper, we discussed the “overshooting” effect in the EXIT chart of ISCD. At first, we identified the reason for this effect. So far, it was common to approximate all input  $L$ -values by the same Gaussian distributed process when determining the EXIT curve of SDDS. No distinction has been made whether these input  $L$ -values represent data bits of the present interleaver block under consideration or of preceding blocks. As a novel solution we proposed to apply two different Gaussian distributed processes to distinguish between data of present and past interleaver blocks. Finally, we demonstrated the extended capabilities of the new approach by simulation.

### REFERENCES

- [1] T. Fingscheidt and P. Vary, “Softbit Speech Decoding: A New Approach to Error Concealment,” *IEEE Trans. Speech Audio Process.*, vol. 9, no. 3, pp. 240–251, Mar. 2001.
- [2] M. Adrat, P. Vary, and J. Spittka, “Iterative Source-Channel Decoder Using Extrinsic Information from Softbit-Source Decoding,” *IEEE ICASSP*, vol. IV, Salt Lake City, Utah, USA, May 2001, pp. 2653–2656.
- [3] N. Görtz, “Iterative Source-Channel Decoding using Soft-In/Soft-Out Decoders,” *IEEE ISIT*, Sorrento, Italy, June 2000, p. 173.
- [4] C. Berrou and A. Glavieux, “Near Optimum Error Correcting Coding and Decoding: Turbo-Codes,” *IEEE Trans. Commun.*, vol. 44, no. 10, pp. 1261–1271, Oct. 1996.
- [5] J. Hagenauer, E. Offer, and L. Papke, “Iterative Decoding of Binary Block and Convolutional Codes,” *IEEE Trans. Inf. Theory*, vol. 42, no. 2, pp. 429–445, Mar. 1996.
- [6] S. ten Brink, “Convergence Behavior of Iteratively Decoded Parallel Concatenated Codes,” *IEEE Trans. Commun.*, vol. 49, no. 10, pp. 1727–1737, Oct. 2001.
- [7] M. Adrat, U. von Agris, and P. Vary, “Convergence Behavior of Iterative Source-Channel Decoding,” *IEEE ICASSP*, vol. IV, Hongkong, China, Apr. 2003, pp. 269–272.
- [8] M. Adrat and P. Vary, “Iterative Source-Channel Decoding: Improved System Design Using EXIT Charts,” *EURASIP J. Appl. Signal Process.; Special Issue Turbo Process.*, vol. 2005, no. 6, pp. 928–941, May 2005.
- [9] M. Adrat, P. Vary, and T. Clevorn, “Optimized Bit Rate Allocation for Iterative Source-Channel Decoding and its Extension towards Multi-Mode Transmission,” *IST Mobile & Wireless Commun. Summit*, Dresden, Germany, June 2005.
- [10] A. Q. Pham, L. L. Yang, and L. Hanzo, “Iterative Source and Channel Decoding Using Over-Complete Source Mapping,” *IEEE VTC-Fall*, Baltimore, MD, USA, 2007, pp. 1072–1076.
- [11] R. Thobaben, “A New Transmitter Concept for Iteratively-Decoded Source-Channel Coding Schemes,” *IEEE Workshop on Signal Processing Advances in Wireless Communications (SPAWC)*, Helsinki, Finland, 2007.
- [12] M. Adrat, J. Brauers, T. Clevorn, and P. Vary, “The EXIT-Characteristic of Softbit-Source Decoders,” *IEEE Commun. Lett.*, vol. 9, no. 6, pp. 540–542, June 2005.
- [13] T. Clevorn, P. Vary, and M. Adrat, “Parameter SNR Optimized Index Assignments and Quantizers based on First Order A Priori Knowledge for Iterative Source Channel Decoding,” *CISS*, Princeton, New Jersey, USA, Mar. 2006.
- [14] L. R. Bahl, J. Cocke, F. Jelinek, and J. Raviv, “Optimal Decoding of Linear Codes for Minimizing Symbol Error Rate,” *IEEE Trans. Inf. Theory*, vol. 20, no. 2, pp. 284–287, Mar. 1974.
- [15] M. Adrat, T. Clevorn, and L. Schmalen, “Iterative Source-Channel Decoding & Turbo DeCodulation,” *Advances in Digital Speech Transmission*, R. Martin, U. Heute, and C. Antweiler, Eds. John Wiley & Sons, Ltd., Jan. 2008, ch. 13, pp. 365–398.